Lecture notes on Floquet theory, SS2025

Milena Grifoni
Institute for Theoretical Physics, University of Regensburg

May 9, 2025

Abstract

How to characterize properties of a quantum system subject to an intense time-periodic drive? We shall address this question within the framework of Floquet theory. According to Floquet theorem, the solutions of the time-dependent Schrödinger equation display a quasi-stationary evolution, governed by quasi-energies, and a periodic part. Working in the Sambe space, it is possible to evaluate both the so-called quasi-energy spectrum and the Floquet functions without resorting to perturbation theory in the strength of the time-periodic part of the Hamiltonian or other commonly used approximations. Noticeably, the quasi-energy spectrum can be qualitatively different from the one of the undriven Hamiltonian, opening pathways to manipulate properties of quantum systems by a time-periodic drive.
These concepts will be illustrated on the example of a strongly driven two-level system.

Contents

1 Introduction **2**
- 1.1 Outline . . . 2
- 1.2 Basic literature . . . 2
- 1.3 Floquet theorem . . . 2
  - 1.3.1 Sambe space . . . 3
- 1.4 The driven two-level system . . . 5
  - 1.4.1 Longitudinal two-level system . . . 5
  - 1.4.2 The driven two-level system with longitudinal and transverse coupling 6
  - 1.4.3 Generalized rotating wave approximation . . . 8
  - 1.4.4 Van Vleck perturbation theory . . . 8
- 1.5 Dynamics . . . 9
  - 1.5.1 Coherent destruction of tunneling . . . 11
  - 1.5.2 Driving induced coherent oscillations . . . 12
  - 1.5.3 Conventional Rabi oscillations . . . 12
- 1.6 Comparison with experiments . . . 13

Chapter 1

Introduction

1.1 Outline

How to steer and characterize properties of matter by a time-periodic drive, e.g. intense microwave or optical fields, has been object of investigation since the early days of quantum mechanics. Nowadays pathways to manipulate material properties by a time-periodic drive are often dubbed as Floquet engineering. They are based on the observation that the time evolution and steady state of a quantum system under time-periodic driving can be described in terms of a Floquet Hamiltonian, whose quasi-eigenenergy spectrum can be entirely different from the spectrum of the undriven Hamiltonian. In these notes we shall introduce the basics of Floquet theory and discuss its applications to the simple yet not trivial case of a driven two-level system. The outline is as follows:

1. Floquet theorem

2. The driven two-level system

1.2 Basic literature

- J. H. Shirley, *Solution of the Schrdinger equation with a Hamiltonian periodic in time*, Phys. Rev. **138** B979 (1965)

- J.Hausinger and M. Grifoni, *Dissipative two-level system under strong ac driving: A combination of Floquet and Van Vleck perturbation theory*, Phys. Rev. A **81** , 022117 (2010).

1.3 Floquet theorem

Consider the time-dependent Schrödinger equation

$$i\hbar\partial_t|\psi(t)\rangle = \hat{H}(t)|\psi(t)\rangle\,, \tag{1.1}$$

for a Hamiltonian being periodic in time

$$\hat{H}(t+T) = \hat{H}(t)\,, \quad T = 2\pi/\omega\,. \tag{1.2}$$

Then Floquet theorem states that the Schrödinger equation is solved by

$$|\psi_\alpha(t)\rangle = e^{-iE_\alpha t/\hbar}|u_\alpha(t)\rangle\,, \tag{1.3}$$

where $|u_\alpha(t+T)\rangle = |u_\alpha(t)\rangle$ are periodic in time and called Floquet functions. The quasi-energies $E_\alpha \in \mathbb{R}$ are real parameters, as ensured by the hermiticity of $\hat{H}$; they contribute a phase to the time-evolution, as the energies do for time-independent problems. The Floquet factors and the quasi-energies are obtained as eigenfunctions and eigenvalues, respectively, of the Floquet Hamiltonian:

$$\mathcal{H}_F(t)|u_\alpha(t)\rangle = \left[\hat{H}(t) - i\hbar\partial_t\right]|u_\alpha(t)\rangle = E_\alpha|u_\alpha(t)\rangle\,, \tag{1.4}$$

as it soon follows by inserting Eq. (1.3) in the time-dependent Schrödinger equation. Note that $|u_{\alpha,n}(t)\rangle \equiv e^{-in\omega t}|u_\alpha(t)\rangle$ yields a solution of Eq. (1.1) physically identical to Eq. (1.3) but with shifted eigenenergies $E_{\alpha,n} \equiv E_\alpha - \hbar n\omega$. Furthermore, $E_{\alpha,0} = E_\alpha$ and $|u_{\alpha,0}(t)\rangle = |u_\alpha(t)\rangle$. Hence, it will be sufficient to examine the set of eigenvalues $\{E_{\alpha,n}\}$ with $-\hbar\omega/2 \le E_{\alpha,n} \le \hbar\omega/2$. In the following we look for solutions of the Floquet equation

$$\mathcal{H}_F(t)|u_{\alpha,n}(t)\rangle = E_{\alpha,n}|u_{\alpha,n}(t)\rangle\,. \tag{1.5}$$

Notice that the quasi-energy spectrum can exhibit degeneracies any time that one satisfies the condition

$$E_{\alpha,n} = E_{\beta,m}\,, \quad \alpha \neq \beta\,, \, m \neq n\,. \tag{1.6}$$

This equality can be interpreted as a resonance induced by the absorption or emission of photons. Such resonance is shown in Fig. 1.1 for the case of a longitudinally driven two-level system (TLS).

1.3.1 Sambe space

The strength of Floquet theory is to enable one to recast the time-dependent Floquet equation for vectors leaving in the Hilbert space $\mathcal{H}$ into a time-independent problem in the larger Sambe space $\mathcal{S} = \mathcal{H} \otimes \mathcal{T}$, where $\mathcal{T}$ is the Hilbert space of the T-periodic functions. In particular, the inner product in $\mathcal{T}$ is defined as

$$(f, g) := \frac{1}{T}\int_0^T dt f^*(t)g(t)\,. \tag{1.7}$$

The functions $\{\varphi_l(t) = e^{-il\omega t}\,, l \in \mathbb{Z}\}$ build a complete set of $\mathcal{T}$, where we further define for a basis-independent notation the state vectors $|l)$, with $\varphi_l(t) = (t|l)$ and $\varphi_l^*(t) = (l|t)$. Furthermore, the completeness and orthogonality relations are

$$\frac{1}{T}\int_0^T dt|t)(t| = 1\,, \quad \sum_l |l)(l| = 1\,, \tag{1.8}$$

and

$$(t|t') = \delta(t-t')\,, \quad , \quad (l|m) = \delta_{l,m}\,. \tag{1.9}$$

respectively.
In the extended Sambe space $\mathcal{S} = \mathcal{H} \otimes \mathcal{T}$ vectors are indicated as $|\cdot\rangle\rangle$, with $|u_\alpha(t)\rangle = (t|u_\alpha\rangle\rangle$; the inner product is defined as

$$\langle\langle\cdot|\cdot\rangle\rangle := \frac{1}{T}\int_0^T dt \langle\cdot|\cdot\rangle\,. \tag{1.10}$$

Consider now a generic time-periodic Floquet vector $|u_{\alpha,n}(t)\rangle$ leaving in the Hilbert space $\mathcal{H}$. We can expand it in Fourier series, thus getting an expansion in basis functions of $\mathcal{T}$. We otain

$$|u_{\alpha,n}(t)\rangle = \sum_{l'} e^{i(l'-n)\omega t}|u_\alpha^{(l')}\rangle = \sum_l e^{-il\omega t}|u_\alpha^{(n-l)}\rangle\,, \tag{1.11}$$

where $|u_\alpha^{(k)}\rangle$ are Fourier coefficients. In the composite Sambe space we define

$$|u_{\alpha,n}\rangle\rangle \equiv \sum_l |u_\alpha^{(n-l)}\rangle \otimes |l)\,, \tag{1.12}$$

such that $|u_{\alpha,n}(t)\rangle = (t|u_{\alpha,n}\rangle\rangle$.
In the Sambe space the Floquet Hamiltonian is an infinite matrix. Furtermore, it is diagonal in the basis spanned by the vectors $\{|u_{\alpha,n}\rangle\rangle\}$, and with entries provided by the quasi-energies $E_{\alpha,n}$.

Note: Fourier expansion

The Floquet vector can be be further spanned by the basis vectors $\{|\nu\rangle\}$, where ν indicates a collective set of quantum numbers. Then it holds in the basis $\{|\nu\rangle\}$ the expansion

$$|u_\alpha(t)\rangle = \sum_\nu c_\nu^\alpha(t)|\nu\rangle\,, \quad c_\nu^\alpha(t+T) = c_\nu^\alpha(t)\,, \tag{1.13}$$

whereby

$$c_\nu^\alpha(t) = \langle\nu|u_\alpha(t)\rangle\,. \tag{1.14}$$

We can expand the coefficients $c_\nu^\alpha(t)$ in Fourier series. This yields

$$|u_\alpha(t)\rangle = \sum_\nu c_\nu(t)|\nu\rangle = \sum_l \sum_\nu c_{\nu,l}^\alpha e^{-il\omega t}|\nu\rangle\,, \tag{1.15}$$

where

$$c_{\nu,l}^\alpha = (\varphi_l, c_\nu^\alpha) = \frac{1}{T}\int_0^T dt e^{il\omega t} c_\nu^\alpha(t) \tag{1.16}$$

are the time-independent Fourier coefficients in an expansion of the vector $|u_\alpha(t)\rangle$. At the same time, we can work in the Sambe space and define the vectors

$$|u_\alpha\rangle\rangle \equiv \sum_l \sum_\nu c_{\nu,l}^\alpha|\nu\rangle \otimes |l) = \sum_l \sum_\nu c_{\nu,l}^\alpha|\nu,l\rangle\rangle\,, \tag{1.17}$$

such that $|u_\alpha(t)\rangle = (t|u_\alpha\rangle\rangle$, and

$$c^\alpha_{\nu,l} = \langle\langle \nu, l|u_\alpha\rangle\rangle = \frac{1}{T}\int_0^T dt e^{il\omega t}\langle\nu|u_\alpha(t)\rangle = \frac{1}{T}\int_0^T dt\langle\nu|u_{\alpha,-l}(t)\rangle\,. \tag{1.18}$$

1.4 The driven two-level system

As a first example we investigate a two-level system (TLS), i.e., a quantum system with two relevant states, subject to periodic driving. It can describe e.g. a spin 1/2 in oscillating magnetic field, a two-level atom in an electric field, or any kind of quantum bit (qubit) subject to a time-periodic drive. We first consider the exactly solvable case of driving being diagonal in the eigenbasis of the undriven system. Then we turn to the generic case in which the system is no longer exactly solvable due to an additional transverse coupling.

1.4.1 Longitudinal two-level system

Let us start by considering the driven two-level Hamiltonian

$$\hat{H}_{\mathrm{TLS}}(t) = \hat{H}_0 + \hat{V}(t) = -\frac{\hbar}{2}(\varepsilon + A\cos\omega t)\sigma_z\,, \tag{1.19}$$

with σ_z the diagonal Pauli matrix, and longitudinal bias consisting of the dc component ε and a sinusoidal modulation of amplitude A and frequency ω. In the absence of the periodic drive, $A = 0$, is $\hat{H}_{\mathrm{TLS}}(t) = \hat{H}_0$, with eigenstates $|\uparrow\rangle$, $|\downarrow\rangle$ being the eigenstates of σ_z with eigenvalues $\sigma = \pm 1$, respectively. Explicitly, $\sigma_z|\uparrow\rangle = +|\uparrow\rangle$, $\sigma_z|\downarrow\rangle = -|\downarrow\rangle$.
For finite driving, $A \neq 0$, the solutions of the TDSE have the form

$$|\psi_\sigma(t)\rangle = e^{i\sigma\left(\frac{1}{2}\varepsilon t + \frac{A}{\omega}\sin\omega t\right)}|\sigma\rangle\,, \quad \sigma = \pm \,\mathrm{or}\, (\downarrow,\uparrow)\,. \tag{1.20}$$

Here is meant that the eigenvalues take the value ± 1 but the states or eigenvalues are indexed through the spin. Hence the Floquet states and quasi-energies are, respectively,

$$|u_{\sigma,n}(t)\rangle = |\sigma\rangle e^{i\sigma\frac{A}{\omega}\sin\omega t}e^{-in\omega t}\,, \quad E_{\sigma,n} = -\sigma\hbar\varepsilon/2 - n\hbar\omega\,. \tag{1.21}$$

We can use the expansion of the periodic term in Bessel functions,

$$e^{i\sigma\frac{A}{\omega}\sin\omega t} = \sum_k e^{i\sigma k\omega t}J_k\left(\frac{A}{2\omega}\right)\,, \tag{1.22}$$

where $J_k(x)$ is the k-th Bessel function of the first kind, to express the above states in the Sambe space. It holds

$$|u_{\sigma,n}\rangle\rangle = |\sigma\rangle\sum_l J_{\sigma(n-l)}\left(\frac{A}{2\omega}\right)|l)\,. \tag{1.23}$$

The quasi-energy spectrum of the driven TLS is shown in Fig. 1.1 as a function of the static bias. It exhibits exact degeneracies any time that one satisfies the condition

$$E_{\sigma,n} = E_{\bar{\sigma},m}\,, \quad m \neq n \quad \Leftrightarrow \varepsilon = m\omega\,. \tag{1.24}$$

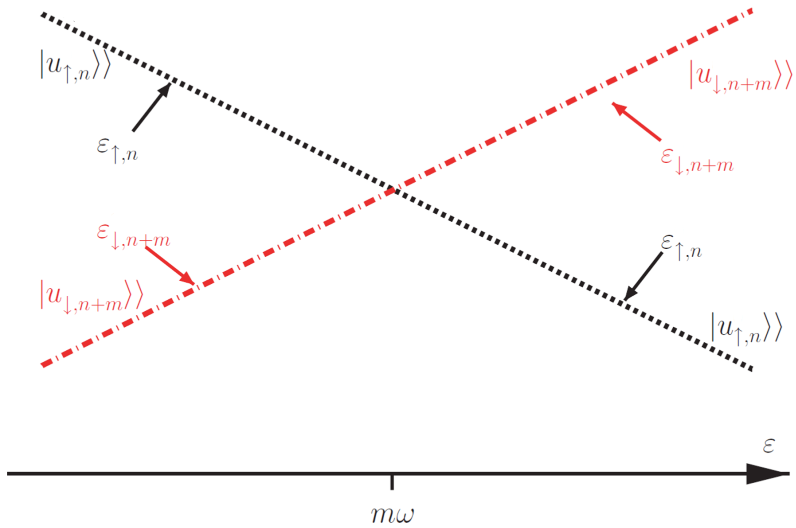

Figure 1.1: Exact crossing in the Floquet spectrum of a longitudinally driven TLS against static bias.

This equality can be interpreted as a resonance induced by the absorption or emission of photons. Such resonance is shown in Fig. 1.1 for the case of a longitudinally driven two-level system (TLS). In the figure and for later use the notation $E_{\sigma,n} = \hbar\varepsilon_{\sigma,n}$ is used. Additionally, $\varepsilon_{\sigma,0} = \varepsilon_\sigma$. Notice that $\varepsilon_{\downarrow,n} - \varepsilon_{\uparrow,m} = \varepsilon - (m-n)\omega$. Hence, $\varepsilon_{\downarrow,1} - \varepsilon_{\uparrow,0} = \varepsilon - \omega$.

1.4.2 The driven two-level system with longitudinal and transverse coupling

We turn to the action of a transverse coupling, e.g. caused, for a spin 1/2 system, by an external magnetic field. The driven Hamiltonian reads

$$\hat{H}_{\mathrm{TLS}}(t) = -\frac{\hbar}{2}[\Delta\sigma_x + (\varepsilon + A\cos\omega t)\sigma_z]\,, \tag{1.25}$$

where σ_z and σ_x are the Pauli matrices, and as basis states we choose the eigenstates $|\uparrow\rangle$, $|\downarrow\rangle$ of σ_z. The coupling strength Δ between those two basis states is time independent, whereas the bias point consists of the dc component ε and a sinusoidal modulation of the amplitude A and frequency ω. Noticeably, despite its apparent simplicity, such Hamiltonian cannot be solved exactly!

Let us now get advantage of the periodicity of the driving and work in the Sambe space,

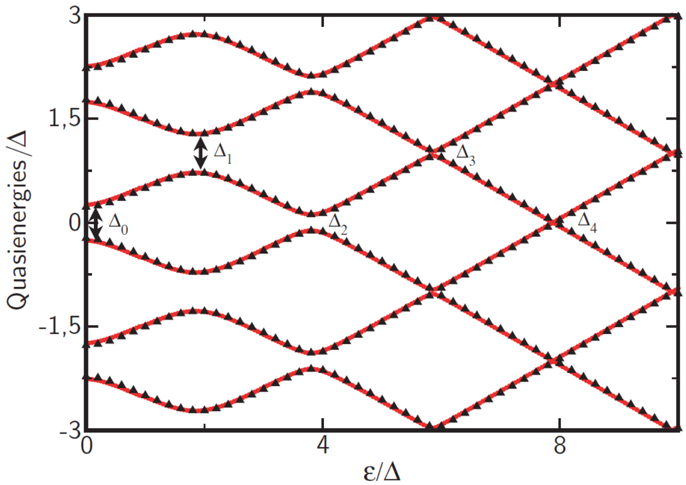

Figure 1.2: Floquet spectrum of a driven TLS against static bias. One notices the occurrence of avoided crossings at the m-th photon resonance of magnitude Δ_n. Parameters are $\omega = 2\Delta$, $A = 3\Delta$.

with basis states $\{|u_{\sigma,n}\rangle\rangle\}$. It holds for the Floquet Hamiltonian,

$$\mathcal{H}_{\text{TLS}} = \hbar \left(\begin{array}{c|cccccc|c} \ddots & |u_{\uparrow,n}\rangle\rangle & |u_{\downarrow,n}\rangle\rangle & |u_{\uparrow,n+1}\rangle\rangle & |u_{\downarrow,n+1}\rangle\rangle & |u_{\uparrow,n+2}\rangle\rangle & |u_{\downarrow,n+2}\rangle\rangle & \\ \hline |u_{\uparrow,n}\rangle\rangle & \varepsilon_{\uparrow,n} & -\frac{1}{2}\Delta_0 & 0 & -\frac{1}{2}\Delta_{-1} & 0 & -\frac{1}{2}\Delta_{-2} & \\ |u_{\downarrow,n}\rangle\rangle & -\frac{1}{2}\Delta_0 & \varepsilon_{\downarrow,n} & -\frac{1}{2}\Delta_1 & 0 & -\frac{1}{2}\Delta_2 & 0 & \\ |u_{\uparrow,n+1}\rangle\rangle & 0 & -\frac{1}{2}\Delta_1 & \varepsilon_{\uparrow,n+1} & -\frac{1}{2}\Delta_0 & 0 & -\frac{1}{2}\Delta_{-1} & \\ |u_{\downarrow,n+1}\rangle\rangle & -\frac{1}{2}\Delta_{-1} & 0 & -\frac{1}{2}\Delta_0 & \varepsilon_{\downarrow,n+1} & -\frac{1}{2}\Delta_1 & 0 & \\ |u_{\uparrow,n+2}\rangle\rangle & 0 & -\frac{1}{2}\Delta_2 & 0 & -\frac{1}{2}\Delta_1 & \varepsilon_{\uparrow,n+2} & -\frac{1}{2}\Delta_0 & \\ |u_{\downarrow,n+2}\rangle\rangle & -\frac{1}{2}\Delta_{-2} & 0 & -\frac{1}{2}\Delta_{-1} & 0 & -\frac{1}{2}\Delta_0 & \varepsilon_{\downarrow,n+2} & \\ \hline & & & & & & & \ddots \end{array}\right) \tag{1.26}$$

with $E_{\sigma,n} = \hbar\varepsilon_{\sigma,n}$ and where we defined

$$\Delta_{n-l} \equiv \Delta\langle\langle u_{\uparrow,n}|\sigma_x|u_{\downarrow,l}\rangle\rangle = J_{n-l}\left(\frac{A}{2\omega}\right)\Delta\,. \tag{1.27}$$

In the following we call $|\Phi_{\alpha,n}\rangle\rangle$ the Floquet functions diagonalizing the Floquet Hamiltonian Eq. (1.26), with $\alpha = \pm$. Approximate forms will be discussed in the next subsection. The resulting Floquet spectrum is shown in Fig. 1.2. We notice now the occurrence of avoided crossing at the position where the longitudinally driven TLS had exact crossings. Noticeably, the avoided crossings are given by the dressed tunneling splittings, and hence their magnitude depends on the ratio A/ω.

1.4.3 Generalized rotating wave approximation

When looking at the spectrum of the unperturbed system, $\Delta = 0$, the system is resonant any time the dc-bias fulfills the condition $\varepsilon = m\omega$. As long as the transverse coupling is a small perturbation $\omega, \gg \Delta$, then $\mathcal{H}_{\rm TLS}$ will exhibit a similar energy spectrum. The largest corrections come from the matrix elements connecting the (almost) degenerate levels. Hence, in first approximation, we can diagonalize an effective 2×2 Hamiltonian of the kind

$$\mathcal{H}^{\rm eff}_{\rm TLS} = \hbar \begin{pmatrix} \varepsilon_{\uparrow,n} & -\frac{1}{2}\Delta_{-m} \\ -\frac{1}{2}\Delta_{-m} & \varepsilon_{\downarrow,n+m} \end{pmatrix} . \tag{1.28}$$

One finds the eigenergies

$$\hbar\varepsilon^{\rm RWA}_{-,n} = \hbar[(-n - \frac{1}{2}m)\omega - \frac{1}{2}\Omega^{\rm RWA}_m] , \tag{1.29}$$

$$\hbar\varepsilon^{\rm RWA}_{+,n+m} = \hbar[(-n - \frac{1}{2}m)\omega + \frac{1}{2}\Omega^{\rm RWA}_m] \tag{1.30}$$

with the frequency

$$\Omega^{\rm RWA}_m = \sqrt{(-\varepsilon + m\omega)^2 + \Delta^2_{-m}} . \tag{1.31}$$

The corresponding eigenstates are

$$|\Phi^{\rm RWA}_{-,n}\rangle\rangle = -\sin\frac{\theta_m}{2}|u_{\uparrow,n}\rangle\rangle - \mathrm{sgn}(\Delta_{-m})\cos\frac{\theta_m}{2}|u_{\downarrow,n+m}\rangle\rangle , \tag{1.32}$$

$$|\Phi^{\rm RWA}_{+,n+m}\rangle\rangle = \cos\frac{\theta_m}{2}|u_{\uparrow,n}\rangle\rangle - \mathrm{sgn}(\Delta_{-m})\sin\frac{\theta_m}{2}|u_{\downarrow,n+m}\rangle\rangle , \tag{1.33}$$

where $\tan\theta_m = \frac{|\Delta_{-m}|}{-\varepsilon+m\omega}$ for $0 < \theta_m \leq \pi$. The quasi-energy spectrum in the RWA near the resonance is shown in Fig. (1.3).

1.4.4 Van Vleck perturbation theory

Besides the simple RWA, also more sophisticated approximation schemes can be used if one wants to account for higher order effects in Δ, such as a shift in the oscillation frequency Ω_m or, in the presence of dissipation, the correct order of magnitude of the relaxation and dephasing rates [2]. The method of choice is for this case Van Vleck perurbation theory (VVPT). A unitary transformation $\hat{U} = e^{i\hat{S}}$ is applied in order to construct an effective Hamiltonian which exhibits, to a certain order in the perturbation, the same eigenenergies as the original Hamiltonian but only connects almost degenerate levels. In the case of the Floquet Hamiltonian, the effective Hamiltonian then becomes $\mathcal{H}^{\rm eff}_{\rm VV} = \exp(i\hat{S})\mathcal{H}_{\rm TLS}\exp(-i\hat{S})$, with the transformation matrix $\hat{S}$ evaluated up to a given order order in Δ. The so-obtained effective Hamiltonian for an m-photon resonance again consists of 2×2 blocks; however, compared to the one of the previous section, it has corrected diagonal entries. For example, within *second order* VVPT, we find

$$\mathcal{H}^{\rm eff}_{\rm VV} = \hbar \begin{pmatrix} \varepsilon_{\uparrow,n} - \frac{1}{4}\sum_{l\neq -m}\frac{|\Delta_l|^2}{\varepsilon+l\omega} & -\frac{1}{2}\Delta_{-m} \\ -\frac{1}{2}\Delta_{-m} & \varepsilon_{\downarrow,n+m} + \frac{1}{4}\sum_{l\neq -m}\frac{|\Delta_l|^2}{\varepsilon+l\omega} \end{pmatrix} . \tag{1.34}$$

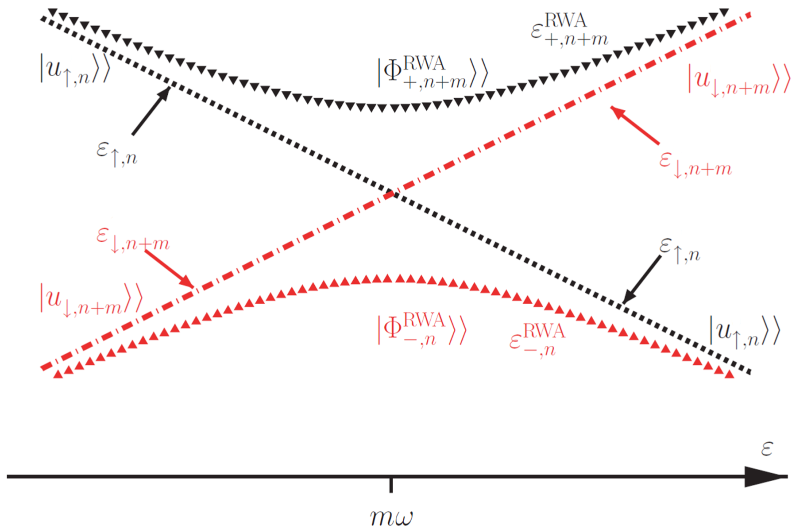

Figure 1.3: Floquet spectrum of a driven TLS in the rotating-wave approximation against static bias.

The above correction $\delta_m = \frac{1}{4}\sum_{l\neq -m}\frac{|\Delta_l|^2}{\varepsilon+l\omega}$ in turn affects the resonance condition, the oscillation frequency and the eigenvectors. Specifically, the RWA formulas remain valid upon the replacements $\varepsilon = m\omega \to \varepsilon = m\omega - 2\delta_m$, $\Omega_m \to \Omega_m^{\rm VV}$, $\theta_m \to \theta_m^{\rm VV}$, respectively.

1.5 Dynamics

The properties of the driven TLS are conveniently described in terms of the density operator $\hat{\rho}(t)$. In the Floquet basis, it holds

$$\rho_{\alpha,\beta}(t) = \langle \Phi_\alpha(t)|\hat{\rho}(t)|\Phi_\beta(t)\rangle\,, \quad \alpha,\beta = \pm\,, \tag{1.35}$$

whereby $\rho_{+,+}(t)+\rho_{-,-}(t) = 1$ for all t, and $\rho_{-,+}(t) = \rho^*_{+,-}(t)$. We assume that at time $t=0$ the system was prepared in the state $|\downarrow\rangle$. In other words, at time $t=0$ the density operator is described by the pure state $\hat{\rho}(t=0) = |\downarrow\rangle\langle\downarrow|$. The observable of interest, relevant also in qubit experiments, is taken to be the survival probability

$$P_{\downarrow\to\downarrow}(t) = \langle\downarrow|\hat{\rho}(t)|\downarrow\rangle\,. \tag{1.36}$$

The transition probability is in turn $P_{\downarrow\to\uparrow} = 1 - P_{\downarrow\to\downarrow}$. From the physical point of view, the system is prepared in a state which is not the eigenstate of the full Hamiltonian, and hence coherent oscillations are expected. Importantly, the period of the oscillations will depend in a non trivial way on both the couplings Δ_m, the driving frequency ω and the amplitude A. In order to find the density operator, we simply look at the differential equation it obeys. From the Floquet equation it soon follows

$$\dot{\rho}_{\alpha,\beta}(t) = -i(\varepsilon_\alpha - \varepsilon_\beta)\rho_{\alpha,\beta}(t)\,, \tag{1.37}$$

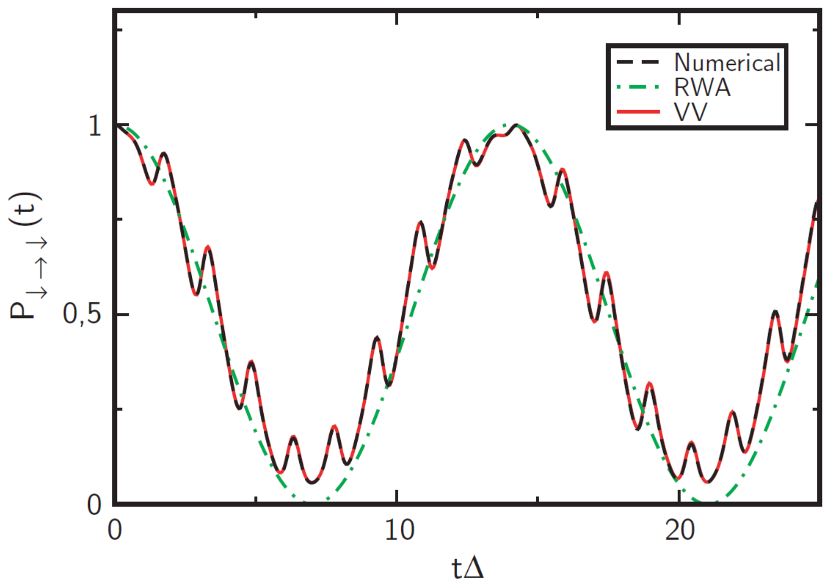

Figure 1.4: Survival probability of a driven TLS in the rotating-wave approximation against Van Vleck perurbation theory and the exact numerical solution. Parameters are $\varepsilon/\Delta = 4$, $\omega/\Delta = 4$ and $A/\Delta = 4.1$.

so that

$$\begin{aligned} \rho_{\alpha,\alpha}(t) &= \rho_{\alpha,\alpha}(0)\,, \\ \rho_{\alpha,\beta}(t) &= \rho_{\alpha,\beta}(0)e^{-i(\varepsilon_\alpha-\varepsilon_\beta)t} \quad \alpha\neq\beta\,. \end{aligned} \tag{1.38}$$

The starting conditions are calculated through

$$\rho_{\alpha,\beta}(0) = \langle\Phi_\alpha(0)|\downarrow\rangle\langle\downarrow|\Phi_\beta(0)\rangle\,. \tag{1.39}$$

Plugging the above solution in the definition of the survival probability, we obtain

$$P_{\downarrow\to\downarrow}(t) = \langle\downarrow|\hat\rho(t)|\downarrow\rangle = \sum_{\alpha,\beta}\rho_{\alpha,\beta}(t)\langle\downarrow|\Phi_\alpha(t)\rangle\langle\Phi_\beta(t)|\downarrow\rangle\,. \tag{1.40}$$

With focus on an m-photon resonance and using the RWA, it holds

$$\rho_{-,+}(t) = \rho_{-,+}(0)e^{-i(m\omega+\Omega_m)t}\,. \tag{1.41}$$

with $\Omega_m = \sqrt{(-\varepsilon+m\omega)^2+\Delta_{-m}^2}$. Using the above formulas, one finds

$$P^{\rm RWA}_{\downarrow\to\downarrow}(t) = \cos^2(\Omega_m t/2) + \cos^2\theta_m\sin^2(\Omega_m t/2)\,, \tag{1.42}$$

showing that the system displays oscillations with frequency Ω_m. For the case of the exact RWA resonance $\varepsilon = m\omega$ and finite Δ_{-m}, the RWA mixing angle is $\theta_m = \pi/2$, and one finds

$$P^{\rm RWA}_{\downarrow\to\downarrow}(t) = \cos^2\left(J_m\left(\frac{A}{\omega}\right)\frac{\Delta}{2}t\right)\,. \tag{1.43}$$

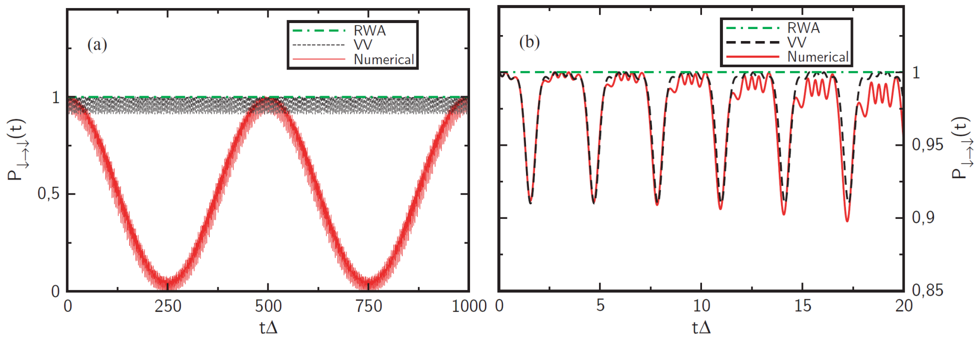

Figure 1.5: Coeherent destruction of tunneling in a driven TLS. The rotating-wave approximation and second order Van Vleck perurbation theory predict exact or strong localization, respectively. The numerical results in contrast show complete population inversion despite with a low oscillation frequency Ω_m. The system is near a three-photon resonance. Parameters are $\varepsilon/\Delta = 6.0$, $\omega/\Delta = 2.0$ and $A/\Delta = 12.7603$.

Hence, we have found that a drive can induce coherent oscillations with a period which depends on how many photons are necessary to achieve the resonance. The oscillation period also depends on how close the system is to the resonance through the detuning δ.
If the Van Vleck perturbation theory is applied up to second, the result above gets modified, in the sense that

$$P^{\mathrm{VV}}_{\downarrow\to\downarrow}(t) = \cos^2(\Omega^{\mathrm{VV}}_m t/2) + \cos^2(\theta^{\mathrm{VV}}_m)\sin^2(\Omega^{\mathrm{VV}}_m t/2) + P^{(1)}_{\downarrow\to\downarrow}(t) + P^{(2)}_{\downarrow\to\downarrow}(t)\,, \tag{1.44}$$

where the last two terms are corrections in first and second order in Δ. As seen in Fig. 1.4, this is reflected in a frequency shift as well as in fast oscillations not visible in the RWA.

1.5.1 Coherent destruction of tunneling

One counterintuitive application of strong driving fields is the possibility to bring the Rabi-like oscillation to a complete standstill by appropriately tuning the drving frequency or its amplitude. This effect goes under the name of coherent destruction of tunneling (CDT). It has been found in [3] for a driven, symmetric double-well potential. The effect was later discussed for driven TLSs. For a symmetric TLS ($\varepsilon = 0$) and for high enough driving frequencies $\omega > \Delta$ this phenomenon was predicted to happen approximately at the zeros of $J_0(A/\omega)$, as can also be seen from Eq. (16). For a nonzero static bias and high frequencies, the necessary conditions for CDT are $\varepsilon = m\omega$ and $J_m(A/\omega) = 0$. The survival probability at the three-photon resonance is shown in Fig. 1.5. It shows a comparison between the RWA and Van Vleck dynamics to second-order and an exact numerical treatment of the Floquet Hamiltonian for the above parameters. For the RWA, we see a complete destruction of tunneling because the driving-induced oscillations are not accounted for. Also, within the Van Vleck description, the coherent oscillations are strongly suppressed; however, we notice fast oscillations because of the external driving. The situation changes strongly for the numerical graph: instead of a localization, a complete inversion of the population occurs; CDTseems

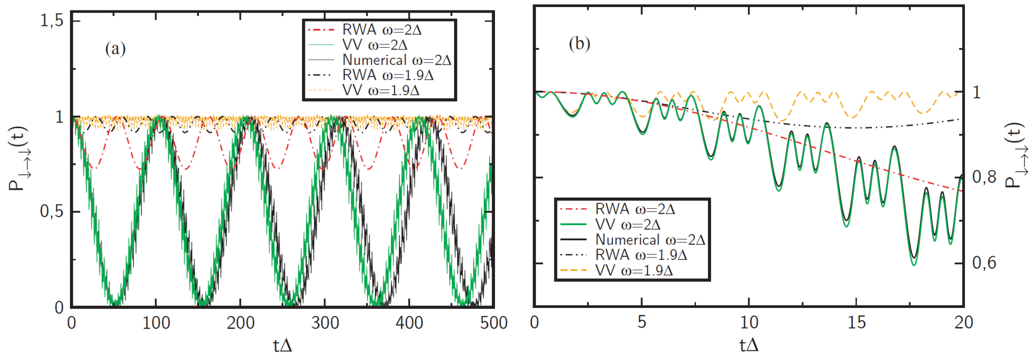

Figure 1.6: Driving-induced tunneling oscillations. Parameters are $\varepsilon/\Delta = 5.9001$ (exact resonance), $\omega/\Delta = 2.0$ and $A/\Delta = 3.0$. Three approaches are compared: a complete numerical solution of the Floquet Hamiltonian, the second-order Van Vleck approach, and the RWA approach. For the first two approaches, complete population inversion is predicted.

to have vanished completely, as the exact oscillation frequency Ω_m is not vanishing. Considering, however, the time scale in Fig. 15(a), we notice that the period is rather large. For short times, see Fig. 1.5(b), also the numerical dynamics appear to be localized.

1.5.2 Driving induced coherent oscillations

An effect contrary to the CDT are driving-induced tunneling oscillations (DITO). It has been predicted, see e.g. in [5], and experimentally shown in [6] for a Cooper pair box, that for a high static energy bias, $\varepsilon \gg \Delta$ and for high driving frequency, $\omega \gg \Delta$, coherent oscillations with frequency $|J_{-m}(A/\omega)|$ and large amplitude are induced if $\varepsilon \approx m\omega$. In a later experiment [7], also based on a Cooper pair box, the full evolution of the resonances was obtained, including the CDT condition. In both [6] and [7] a dressed state approach was used, where the electromagnetic field is quantized.
The DITO are often also named Rabi oscillations even though in the original problem of Rabi [4] a circularly polarized driving field couples to the TLS. As a consequence, the obtained frequency of the oscillations is linear in A. Notice that such linearity of the oscillations with the driving amplitude is also recovered for the longitudinally driven TLS for weak driving fields $A \ll \omega$ and in the vicinity of the first photon resonance $\varepsilon = \omega$. In this case linearization of the first Bessel function predicts in fact

$$J_1(A/\omega) \approx A/\omega\,. \tag{1.45}$$

The driving-induced tunneling oscillations are shown for the case of a three-phonon resonance in Fig. 1.6. For the Van Vleck dynamics one finds the main oscillation frequency $\Omega_3^{\mathrm{VV}} = \Delta|J_{-3}(A/\omega)|$.

1.5.3 Conventional Rabi oscillations

The problem of a driven two-level atom with transverse and longitudinal components was already discussed by Rabi in the late thirties [4]. However, Rabi did not include a static bias

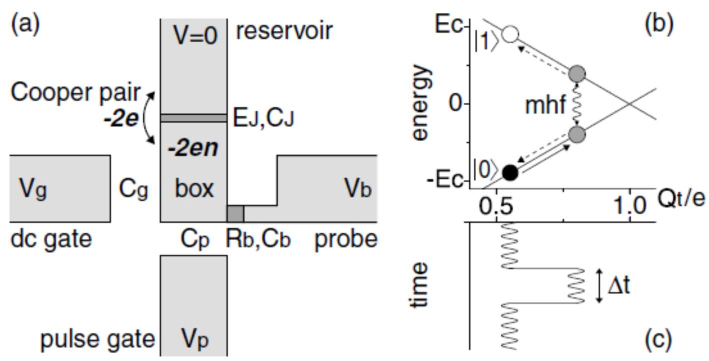

Figure 1.7: (a) Schematic of a Cooper-pair box and an additional probe electrode. (b) Control of the quantum states using Rabi oscillations. The solid lines represent relative energies of two charge states $|0\rangle$ and $|1\rangle$ as a function of total gate-induced charge Q_t . Black circle: initial state. Gray circles: two states under Rabi oscillations. The final state is a superposition of the two states shown by black and white circles. (c) Schematic waveform of the voltage applied to the pulse gate. Figure from [6].

and moreover explicitly considered a *circularly polarized* drive, making the problem exactly solvable. The Rabi Hamiltonian reads

$$\hat{H}^{\mathrm{Rabi}}_{\mathrm{TLS}}(t) = -\frac{\hbar}{2}\Delta\sigma_z - \frac{\hbar}{2}A[\cos(\omega t)\sigma_x + \sin(\omega t)\sigma_y]\,. \tag{1.46}$$

Defining the detuning $\delta = \omega - \Delta$, one gets Rabi oscillations for the survival probability with frequency

$$\Omega^{\mathrm{Rabi}} = \sqrt{\delta^2 + A^2}\,. \tag{1.47}$$

Notice that such Hamiltonian can be obtained starting from Eq. (1.25) for the transverse and longitudinal-driven TLS by setting $\varepsilon = 0$, and performing a rotation of $\pi/2$ which changes $\sigma_z \to \sigma_x$ and $\sigma_x \to \sigma_z$. Furthermore, the additional term proportional to σ_y has to be added. This amounts to start from linearly polarized light and, under the assumption of weak, resonant driving $\omega \approx \Delta$, perform a rotating-wave approximation which neglects counter-rotating terms.
Interestingly, in the Rabi problem only a 1-photon resonance is allowed. The possibility of multiphoton resonances in the longitudinally driven case is ensured by the counter-rotating terms.

1.6 Comparison with experiments

Early experiments proving the strong coupling of a TLS to intense microwave radiation used a Cooper pair box (CPB), a superconducting circuit in which the number of Cooper pairs on the box plays the role of the qubit. Importantly, the TLS parameters can be tuned electrostatically via a gate voltage. The CPB Hamiltonian has the canonical form as in

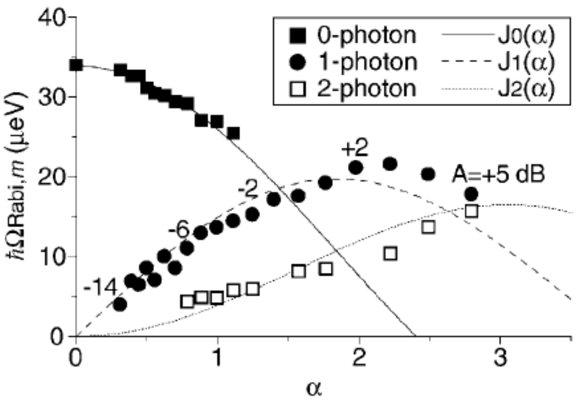

Figure 1.8: Oscillation frequency Ω_m with $m = 0, 1$, and 2, respectively, for 0-, 1-, and 2-photon processes as a function of irradiated microwave amplitude. Lines are the first-kind Bessel functions of the corresponding order, J_m, where α is proportional to the driving amplitude and inversely proportional to the frequency. Data from [6].

Eq. (1.25) upon identifying

$$\hbar\varepsilon = -4E_C(Q_t/e - 1) = , \quad \hbar\Delta = E_J\,, \tag{1.48}$$

with E_J the Josephson coupling energy. The charging energy is provided by the total capacitance C_Σ of the junction and reads $E_C = e^2/C_\Sigma$. The gate induced charge is defined as $Q_t = C_gV_g + C_pV_p + C_bV_b$ and can be tuned through a gate voltage V_g. In the regime $E_C \gg E_J$ the charge representation set by the number states $|0\rangle$, $|1\rangle$ is appropriate. The system is shown in Fig. 1.7. Microwave radiation is then applied to the qubit, hence realizing the model discussed above. The oscillation frequencies at resonance are extracted from oscillations which are recorded upon sweeping a time interval Δt. They are shown in Fig. 1.8. The argument of the Bessel function is proportional to the applied microwave voltage and the inverse of the fre quency, $\alpha = (2eV_{ac}/hf)(C_p/C_\Sigma)$.

Bibliography

[1] J. H. Shirely, *Solution of the Schrdinger equation with a Hamiltonian periodic in time*, Phys. Rev. **138** , B979 (1965).

[2] J.Hausinger and M. Grifoni, *Dissipative two-level system under strong ac driving: A combination of Floquet and Van Vleck perturbation theory*, Phys. Rev. A **81** , 022117 (2010).

[3] F. Grossmann, T. Dittrich, P. Jung, and P. Hänggi, Phys. Rev. Lett. **67**, 516 (1991).

[4] I. I. Rabi, Phys. Rev. **31**, 652 (1937).

[5] L. Hartmann, I. Goychuk, M. Grifoni, and P. Hanggi, Phys. Rev. E **61**, R4687 (2000).

[6] Y. Nakamura, Y. A. Pashkin, and J. S. Tsai, Phys. Rev. Lett. **87**, 246601 (2001).

[7] C. M. Wilson, T. Duty, F. Persson, M. Sandberg, G. Johansson, and P. Delsing, Phys. Rev. Lett. **98**, 257003 (2007).